Submicroscopic Deletions at 13q32.1 Cause Congenital Microcoria

Lucas Fares-Taie,[1] Sylvie Gerber,[1] Akihiko Tawara,[2,20] Arturo Ramirez-Miranda,[3,20] Jean-Yves Douet,[4,20] Hannah Verdin,[5] Antoine Guilloux,[1] Juan C. Zenteno,[6] Hiroyuki Kondo,[2] Hugo Moisset,[1] Bruno Passet,[7] Ken Yamamoto,[8] Masaru Iwai,[9,10] Toshihiro Tanaka,[11,12,13] Yusuke Nakamura,[14] Wataru Kimura,[15] Christine Bole-Feysot,[16] Marthe Vilotte,[7] Sylvie Odent,[17] Jean-Luc Vilotte,[7] Arnold Munnich,[1] Alain Regnier,[4] Nicolas Chassaing,[18] Elfride De Baere,[5] Isabelle Raymond-Letron,[4] Josseline Kaplan,[1] Patrick Calvas,[18] Olivier Roche,[19,21,*] and Jean-Michel Rozet[1,21,*]

Congenital microcoria (MCOR) is a rare autosomal-dominant disorder characterized by inability of the iris to dilate owing to absence of dilator pupillae muscle. So far, a dozen MCOR-affected families have been reported worldwide. By using whole-genome oligonucleotide array CGH, we have identified deletions at 13q32.1 segregating with MCOR in six families originating from France, Japan, and Mexico. Breakpoint sequence analyses showed nonrecurrent deletions in 5/6 families. The deletions varied from 35 kbp to 80 kbp in size, but invariably encompassed or interrupted only two genes: *TGDS* encoding the TDP-glucose 4,6-dehydratase and *GPR180* encoding the G protein-coupled receptor 180, also known as intimal thickness-related receptor (ITR). Unlike TGDS which has no known function in muscle cells, GPR180 is involved in the regulation of smooth muscle cell growth. The identification of a null *GPR180* mutation segregating over two generations with iridocorneal angle dysgenesis, which can be regarded as a MCOR endophenotype, is consistent with the view that deletions of this gene, with or without the loss of elements regulating the expression of neighboring genes, are the cause of MCOR.

Inherited congenital microcoria (MCOR) (MIM 156600), also referred to as congenital miosis, is a rare inborn error of iris development. It is characterized by a small pupil (diameter < 2 mm) that dilates poorly or not at all in response to topically administered mydriatic drugs. Dilation inability results from absent or incompletely developed dilator pupillae muscle. The sphincter pupillae muscle, which acts in opposition to the dilator muscle to cause constriction of the pupil, is unaltered. In addition to abnormal dilator pupillae muscle, the miotic iris is thin and displays abnormal stroma and iridocorneal angle.[1–4] Iris thinning is consistent with transillumination of miotic irises and high sensitivity to light. High myopia and glaucoma are frequently associated with this condition.[5–8]

MCOR is a bilateral disease transmitted as an autosomal-dominant trait with complete penetrance. A unique 8 Mb locus on chromosome 13q31–q32 was mapped in 1998 by linkage analysis[9] in a large multigenerational French pedigree first described in 1964.[10] Gene mapping in some other families confirmed linkage to this locus[11] whereas some others were inconsistent with the 13q31–q32 region, supporting genetic heterogeneity of the disease.[12]

Here, we report a study combining Sanger sequencing and array comparative genomic hybridization (aCGH), which allowed the identification of the molecular defect underlying the disease at the 13q31–32 locus.

We obtained DNA samples of affected and unaffected members of six MCOR-affected families originating from France, Japan, and Mexico (FR1 and FR2, JP1 and JP2, MX1 and MX2, respectively). Three of these families were previously reported (FR1, the original family that allowed mapping of the MCOR locus on chromosome 13q31–q32;[9,10] JP1,[6] and MX1[4]). The pedigrees of the families are presented in Figure 1. The study was approved by ethics committees of each participating institution,

[1]Laboratory of Genetics in Ophthalmology (LGO), INSERM UMR1163, IMAGINE – Institute of Genetic Diseases, Paris Descartes University, 75015 Paris, France; [2]Department of Ophthalmology, University of Occupational & Environmental Health, Kitakyushu 807-8555, Japan; [3]Department of Cornea and Refractive Surgery, Instituto de Oftalmologia "Conde de Valenciana," UNAM, Mexico City, DF 06800, Mexico; [4]Veterinary School of Toulouse, University of Toulouse, 31300 Toulouse, France; [5]Center for Medical Genetics, Ghent University, 9000 Ghent, Belgium; [6]Department of Genetics-Research Unit, Instituto de Oftalmologia "Conde de Valenciana" and Department of Biochemistry, Faculty of Medicine, UNAM, Mexico City, DF 06800, Mexico; [7]UMR1313 Génétique Animale et Biologie Intégrative, Institut Nationale de la Recherche Agronomique, 78352 Jouy-en-Josas, France; [8]Division of Genome Analysis, Institute of Bioregulation, Kyushu University, Fukuoka 812-8582, Japan; [9]Department of Molecular Cardiovascular Biology and Pharmacology, Ehime University Graduate School of Medicine, Ehime 791-0295, Japan; [10]National Hospital Organization, Ehime Medical Center, Tohon, Ehime 791-0281, Japan; [11]Department of Human Genetics and Disease Diversity, Graduate School of Medical and Dental Sciences, Tokyo Medical and Dental University, 113-0034 Tokyo, Japan; [12]Division of Disease Diversity, Bioresource Research Center, Tokyo Medical and Dental University, 113-0034 Tokyo, Japan; [13]Laboratory for Cardiovascular Diseases, RIKEN Center for Integrative Medical Sciences, Yokohama, Kanagawa 230-0045, Japan; [14]Department of Medicine and Surgery, The University of Chicago, Chicago, IL 60637, USA; [15]Kimura Eye Clinic, Kure 737-0046, Japan; [16]Genomics Platform, IMAGINE Foundation and Paris Descartes University, 75015 Paris, France; [17]Service de Génétique Clinique, CHU Hôpital Sud, 35203 Rennes, France; [18]Service de Génétique Clinique, Hôpital Purpan, 31300 Toulouse, France; [19]Department of Ophthalmology, IHU Necker-Enfants Malades, University Paris-Descartes, 75015 Paris, France
[20]These authors contributed equally to this work
[21]These authors contributed equally to this work and are co-senior authors
*Correspondence: oph.roche@free.fr (O.R.), jean-michel.rozet@inserm.fr (J.-M.R.)
http://dx.doi.org/10.1016/j.ajhg.2015.01.014. ©2015 by The American Society of Human Genetics. All rights reserved.

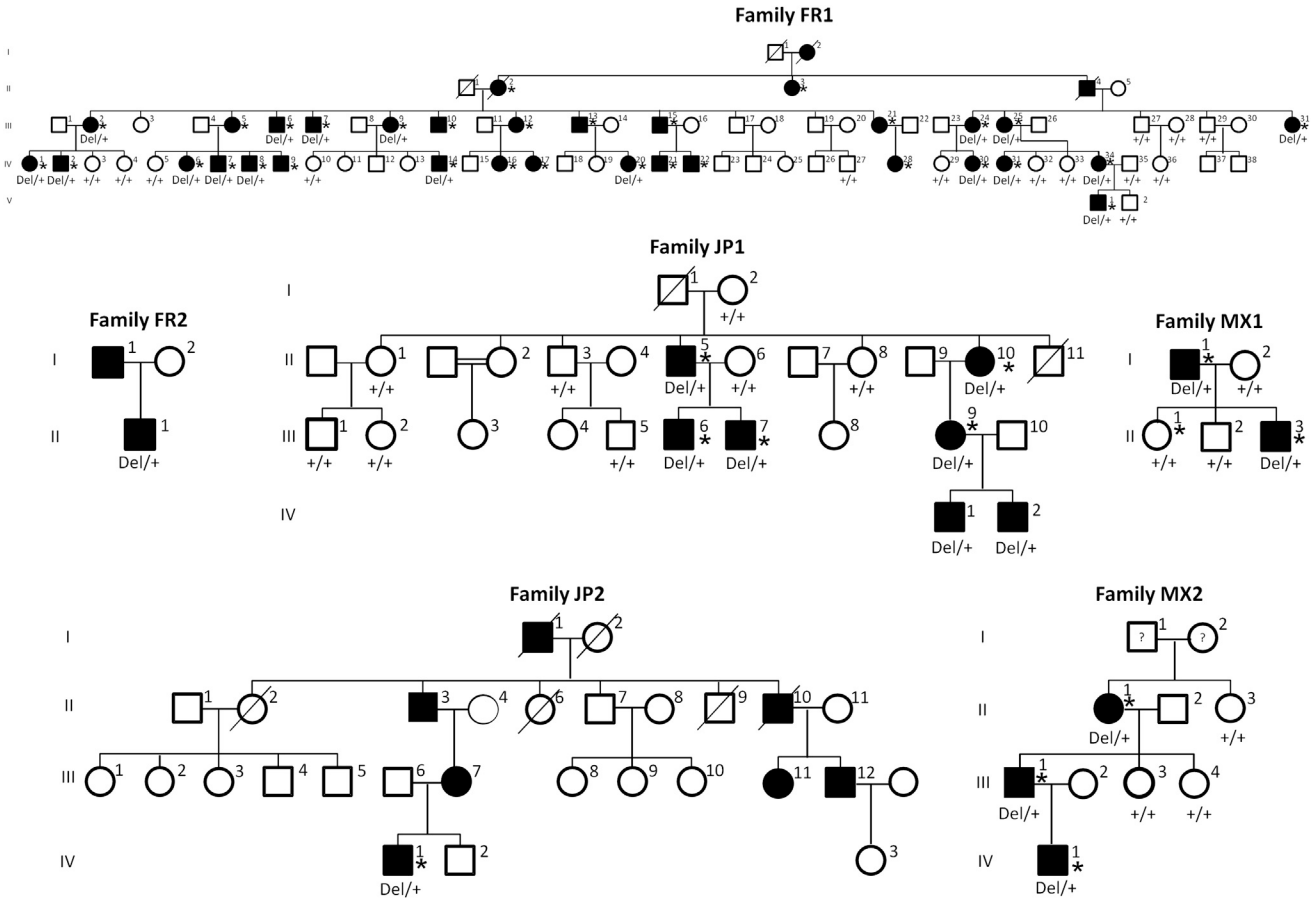

Figure 1. Pedigrees of the Six Families Segregating MCOR
Autosomal-dominant transmission is supported by father-to-son transmission in all six families. Individual numbers in pedigrees FR1[9] and JP1[6] are those previously reported. Available DNA can be identified by the presentation of their genotype at the 13q32.1 locus (Del, deletion; +, wild-type allele). Individuals affected with MCOR who were examined by gonioscopy (asterisk) had all iridocorneal angle dysgenesis.

namely Paris Ile-de-France II; University of Occupational and Environmental Health, Japan; and Instituto de Oftalmologia Conde de Valenciana, Mexico City. Individuals participating to the study provided informed consents for molecular analyses.

Sanger sequencing of the coding region and intron-exon boundaries of genes lying within the 8 Mb MCOR interval on 13q31–q32, and whole-exome sequencing combined with linkage analysis failed to detect candidate disease-causing variants segregating with the disease in families FR1 and JP1, respectively (Table S1, Figure S1). Considering the strong linkage at the locus in FR1 (Zmax = 9.79, $\Theta = 0$),[9] we assumed that the mutation in this family was present in an unscreened region or that it might consist in a genomic rearrangement undetectable by PCR-based screening methods. To assess this latter hypothesis, we subjected the DNA of an affected individual (FR1_III7, Figure 1) to CGH on high-resolution oligonucleotide microarray (Affymetrix Cytogenetics Whole-Genome 2.7M Array). Calculation of test over reference Log2 intensity ratios identified a 54.8 kbp deletion in the 13q32.1 region (Figures 2 and S2). We amplified the junction fragment by subjecting the genomic DNA of the index case to PCR by using primers designed just outside of the predicted deletion boundaries (Table S2, Figure S3). Direct sequencing of the 1.1 kb intervening segment showed that the deletion extended from 95,227,374 to 95,277,864 (positions on chromosome 13 according to the Genome Reference Consortium Human Build 37) with centromeric and telomeric breakpoints in intron 11 and intron 8 of the tail-to-tail genes: TDP-glucose 4,6-dehydratase (*TGDS* [RefSeq accession number NM_014305.2]) and the G protein-coupled receptor 180 (*GPR180* [RefSeq NM_180989.5], also known as intimal-thickness-related receptor, *ITR* [MIM 607787]), respectively (Table 1 and Figure 2).

Interestingly, multiplex PCR of short fluorescent fragments (QMPSF)[13] using primer pairs specific to *GPR180*, *TGDS*, and a control gene (*CFTR* [RefSeq NM_000492.3], Table S3) suggested hemizygosity at 13q32.1 in the other French family as well as the two Japanese and two Mexican MCOR-affected families (Figure S4). In all five families, array CGH confirmed the presence of 13q32.1 deletions, which estimated sizes ranging from 39 kbp to 88.9 kbp (Figure S2). Direct sequencing of intervening segments

Figure 2. Overview of the 13q32.1 Deletions Identified in MCOR
Overview of the 13q32.1 locus (chr13: 95,110,000–95,375,000; hg19) with custom tracks showing the delineated deletions presented in this study (horizontal red bars). At the top, the RefSeq Genes Track is included. In addition, ENCODE and conservation tracks are displayed.

amplified with primers designed just outside of the predicted breakpoints (Table S2) showed that the deletions extended from 95,241,606 to 95,276,905 (35.3 kbp encompassing 4/12 *TGDS* and 7/9 *GPR180* exons), 95,228,262 to 95,300,908 (72.6 kbp encompassing 11/12 *TGDS* exons, *GPR180*, and *mir_562*), 95,236,251 to 95,309,380 (73.1 kbp encompassing 4/12 *TGDS* exons, *GPR180*, *mir_562*, and *5S_rRNA*), and 95,225,217 to 95,305,083 (79.9 kbp encompassing *GPR180*, *mir_562*, and *5S_rRNA*) in families FR2, JP1, JP2, and MX1, respectively (Table 1, Figure 2).

In family MX2, we failed to amplify the intervening segment using primers designed with array CGH data. Considering that MX1 and MX2 families had the same ethnic background and shared the same predicted distal deletion breakpoint (Table 1 and Figure S2), we assumed that both families could have inherited the same deletion by descent and that, in corollary, lack of amplification of the junction fragment in family MX2 could result from incorrectly predicted proximal deletion breakpoint. By using the primers designed to amplify family MX1 junction fragment, we were able to amplify family MX2 intervening segment (Figure S3). Direct sequencing demonstrated that the two families shared the exact same deletion (Table 1 and Figure 2). Analysis of microsatellite markers of chromosome 13q31–q32 showed that the deletion was carried by a common 6.4 Mb haplotype, suggesting that it might have been transmitted within both families by a common ancestor (Figure S5).

Deletion fragment-specific PCR assays based on the amplification of intervening segments in all available DNA samples (see Figure 1) allowed us to confirm the cosegregation of the deletions with the disease in 4/6 families (Figure S3). Segregation analysis could not be performed in families FR2 and JP2 because of a lack of DNA samples. Positive PCR amplification of intragenic *GPR180* fragments confirmed heterozygosity of all deletions (not shown).

The copy-number variations identified in this study are publicly available in the DECIPHER database as 301464, 301465, 301468, 301469, 301471, and 301472. None of them have been previously reported in the DECIPHER database, the Database of Genomic Variants (DGV), or in the cohort of individuals affected with variable diseases analyzed by array CGH at our institute (n = 96; unpublished data). However, chromosome 13q deletions are not uncommon and cause a wide spectrum of phenotypes correlated to the size and position of the deleted region. To our knowledge, microcoria has not been described in individuals with 13q deletions encompassing the 13q32.1 region. However, microcoria could be overlooked or might

Table 1. Summary of 13q32.1 Deletions Identified by Array CGH and Characterized by Sequencing of the Intervening Segments

		Deletions Predicted by Array CGH					Actual Deletions			
		Centromeric Boundaries		Telomeric Boundaries						
Family	Individual	+Probe (position)	−Probe (position)	−Probe (position)	+Probe (position)	Estimated Size (kbp)	Deletion Breakpoints	Size (kbp)	Genes Included or Disrupted by the Deletion	Sequence of the Junction Fragment[a]
FR1	III7	C-08UO9 (95,224,547)	C-08UOA (95,225,723)	S-2NJCM (95,276,735)	C-08UPK (95,279, 378)	54.8	95,227,374–95,277,864	50.5	*TGDS*,[b] *GPR180*[b]	AAAAATCAACTATTTTTTTCTTCTTAACTTCTAA AGTCATTCAATACTGAACTTGGT/**AT**GCAAAT ATGAATGTACATTCTTTTTTCTTTTACAGGAAT ATTACACATTTGTG
FR2	II1	C-3ZRLF (95,238,814)	C-3DRMS (95,238,827)	C-6YHLK (95,277,799)	C-4AEYA (95,277,841)	39.0	95,241,606–95,276,905	35.2	*TGDS*,[b] *GPR180*[b]	TCACCCAGGCTGGAGTGCAGTGGTGCAACC TCAGCTCACTGCAAGCTCTGTCTCCC/**GGG TTCACGCCATTCTCCTGCCTCAGCCTCCC GAGTA**ACTCGCGCCCACGCCCGGCTAAG TTTTTGTATTTTTAGTAGAGACGGGGTTTCA CCG
JP1	IV1	S-4RUHL (95,211,097)	C-7G8VT (95,211,706)	C-5TEUV (95,299,777)	C-5TIVX (95,300,029)	88.9	95,228,262–95,300,908	72.6	*TGDS*,[b] *GPR180*, *mir_562*	ATCATTATTTTACATACATGTAAAAAAGAAAAA AGCTACAATAATAATTATAAGACACCAGT/**G**TC CTCTCTCAGCACAGCAGTTTACTTCTTCAGG GGCAGCAGGAGAATCTCTCTGACTTC
JP2	III7	C-3ERLF (95,238,800)	C-3DRMJ (95,238,827)	S-4OHPW (95,309,706)	C-6MYDV (95,309,751)	70.9	95,236,251–95,309,380	73.1	*TGDS*,[b] *GPR180*, *mir_562*, *5S_rRNA*	CGATGATCAATGTCACTTACAGTAAGAAAAAC CCAAATTAAAAACTCAGAGATAC/TCTCATTCT CCAGCTGAAATTCTCAGAAATAATGTCTATGC CATGTACTTTCCCC
MX1	II3	S-3HRGB (95,218,014)	C-6DQEK (95,219,578)	C-6IBIF (95,305,254)	C-4DJSK (95,305,294)	87.2	95,225,217–95,305,083	79.9	*TGDS*,[b] *GPR180*, *mir_562*, *5S_rRNA*	AACCAACTGAAAGGAGAAAAAAAGTTGATCTT AGTTTATAGATGGATTGGCCTGTTC/**TG**AGCC CCATAACAGTGAGCACCTCTAGCACCTAGGA TGCCAGCTGCATGTAT
MX2	III1	C-7ALKO (95,227,834)	C-3GDLS (95,227,835)	C-6IBIF (95,305,254)	C-4DJSK (95,305,294)	77.5	95,225,217–95,305,083	79.9	*TGDS*, *GPR180*, *mir_562*, *5S_rRNA*	AACCAACTGAAAGGAGAAAAAAAGTTGATCTT AGTTTATAGATGGATTGGCCTGTTC/**TG**AGCC CCATAACAGTGAGCACCTCTAGCACCTAGGA TGCCAGCTGCATGTAT

[a]Sequences shared between the proximal and distal sequences at the junction are underlined. The breakpoint (/) has been arbitrarily placed at the 5′ of the identical sequences. Nucleotide positions refer to the human genome reference sequence (hg19 assembly) available at UCSC Genome Browser.
[b]Partial deletion of the gene (see Figure S2).

not manifest owing to severe eye dysgenesis because about one third of children with 13q deletion syndrome have iris and choroid coloboma, glaucoma, cataracts, and cloudy lenses. Together, these data are consistent with the causality of 13q32.1 deletions in MCOR.

Inspection of sequences surrounding MCOR deletion breakpoints identified a duplicated sequence prone to recurrent nonallelic homologous recombination (NAHR) in a unique family (FR2, 37 bp sequence shared between *TGDS* intron 4 and *GPR180* intron 7 at positions 95,241,662–95,241,698 and 95,276,905–95,276,998, respectively; Figure S6).

Recently, several microhomology-mediated repair mechanisms have been described in the etiology of non-recurrent CNVs in human disease.[14–16] These mechanisms, which are guided by the surrounding genomic architecture, include microhomology-mediated end-joining (MMEJ),[17] fork stalling and template switching (FoSTeS),[18] microhomology-mediated break-induced replication (MMBIR),[19] serial replication slippage (SRS),[20] and break-induced SRS (BISRS).[21] Extensive bioinformatic analysis of MCOR deletion breakpoints and surrounding genomic architecture allowed the identification of perfectly matching 1 or 2 base pairs shared between the proximal and distal sequence at the junctions, sequence motifs, and/or repetitive elements that are likely to stimulate the formation of the 13q32.1 deletions by increasing susceptibility of DNA breakage or promote replication fork stalling (Table S4, Figures S6 and S7). These findings are consistent with the view that microhomology-mediated mechanisms underlie non-recurrent MCOR deletions in families FR1, JP1, JP2, MX1, and MX2.

The minimal common deletion disrupted *GPR180* and *TGDS* (Table 1 and Figure 2), raising the possibility that haploinsufficiency of one or the two genes, or alternatively the loss of regulatory elements, might give rise to the phenotype.

GPR180 encodes a 201-amino-acid G protein-coupled receptor[22] of the Rhodopsin-like receptors family that includes hormones, neurotransmitters, and light receptors, all of which transduce extracellular signals upon interaction with guanine nucleotide-binding proteins and activating ligands.[23] Very little is known about the function of GPR180. However, it has been reported to be produced predominantly in vascular smooth muscle cells where its expression is upregulated in response to experimental injury.[24] The significant suppression of DNA synthesis and inability to produce neointima in response to vascular injury in the $Gpr180^{-/-}$ mouse suggest that upregulation of *Gpr180* signaling contributes to vascular smooth muscle growth.[22] In addition, gene expression profiling in normal human tissues has shown that it is highly expressed in myoepithelia (salivary gland, endomyometrium, prostate, lung, and liver).[25] In the eye, *GPR180* is less abundant than in myoepithelia. However, it is listed in the top 20 genes having a significantly higher expression in the iris compared to the other ocular structures.[26] Hence, considering that the dilator pupillae arises during embryonic life by the differentiation of iris epithelial cells into myoepithelial cells,[27,28] *GPR180* was regarded as a strong candidate MCOR gene.

The $Gpr180^{-/-}$ mouse had resistance to experimental thickening of the intima but normal appearance, growth rate, reproduction, and histology of major organs.[22] We examined $Gpr180^{-/-}$ and $Gpr180^{+/-}$ mice for anterior segment development and iris function. We found that both heterozygote and homozygote *Gpr180*-null eyes were undistinguishable from adult age-matched controls (Figures S8–S10). In particular, we found no iris transillumination and normal drug-mediated mydriasis both in heterozygote and homozygote *Gpr180*-null mice. However, inspection of our in-house exome database (>4,200 exomes) for *GPR180* nonsense or frameshift variants with an acceptable amount of reads (≥10) identified a unique heterozygote *GPR180* nonsense mutation (c.343C>T [p.Gln115*]). This variant was found in our own series of individuals with neonatal retinal dystrophy, namely Leber congenital amaurosis (LCA [MIM 204000]). Interestingly, the ophthalmologic file of the blind individual harboring the p.Gln115* substitution (II2, family FR3; Figure 3) mentioned an abnormal iridocorneal angle at examination of the anterior segment of the eye. The individual, her parents, and her siblings consented to ophthalmological examination and genetic analysis. Iridocorneal angle dysgenesis was evidenced in all family members but the mother and a brother affected with LCA (family FR3; Figure 3). Evidence of father-to-son transmission demonstrated autosomal-dominant transmission of the iridocorneal defect that segregated with the p.Gln115* substitution, independently from the autosomal-recessive retinal disease (Figure 3). Whole-genome SNP genotyping data generated via Affymetrix GeneChip Human Mapping 10K 2.0 Arrays were available in this family. Retrospective analysis for linkage with the autosomal-dominant anterior segment dysgenesis pointed to 15 candidate chromosomal regions, including a region on 13q32.1 containing *GPR180* (Figure S11). Retrospective analysis of exome data found no heterozygote loss-of-function variants in any of these regions other than the *GRP180* p.Gln115* substitution, supporting the role of *GPR180* in the development of the iridocorneal angle. Nevertheless, none of the five individuals with both iridocorneal angle dysgenesis and the p.Gln115* substitution had abnormal pupillary response or iris transillumination. Considering that iridocorneal angle dysgenesis is a constant symptom in congenital microcoria linked to 13q32.1 (31/31, 5/5, 1/1, 2/2, and 3/3 of examined MCOR-affected individuals in families FR1,[5,9] JP1,[6] JP2, MX1, and MX2, respectively; Figures 1 and 3), goniodysgenesis in family FR3 can be regarded as a MCOR endophenotype.

The reason why heterozygosity for the p.Gln115* substitution was not sufficient to cause the full range of MCOR symptoms could reside in the production of a truncated protein retaining some of its function. Alternatively,

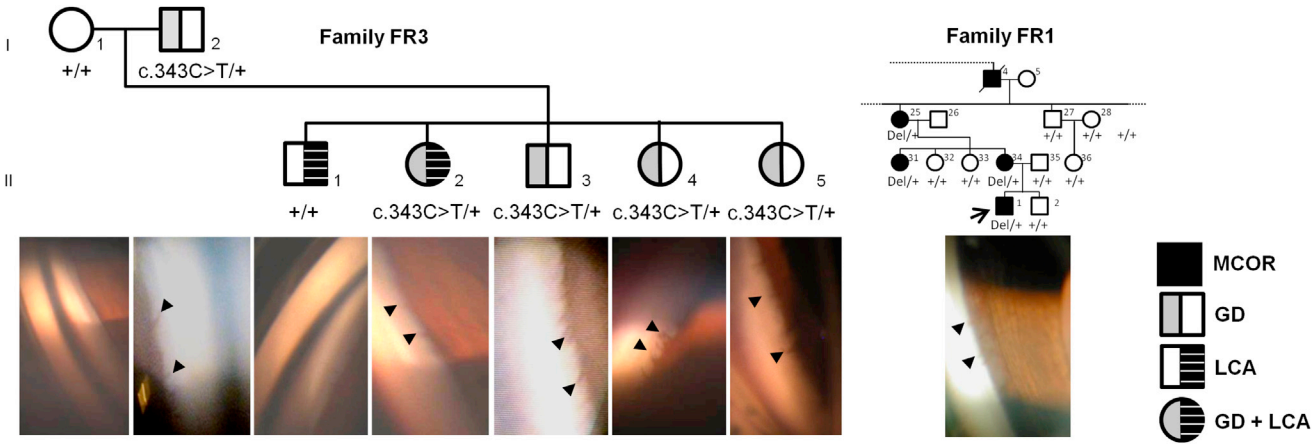

Figure 3. Pedigree, *GPR180* Genotypes, and Gonioscopic Aspects in Families FR3 and FR1
The iris spicules (arrows) consistent with an abnormal development of the iridocorneal angle are seen in individuals harboring the *GPR180* c.343C>T (p.Gln115*) mutation only as well as in individual FR1_V1 affected with microcoria. Abbreviations are as follows: MCOR, microcoria; GD, goniodysgenesis; LCA, Leber congenital amaurosis.

premature termination codon (PTC) self-correcting mechanisms could be involved, in particular translational read-through that has recently been reported to be more abundant than expected in higher species, including human.[29] Nonsense-associated altered splicing (NAS), which consists of selective exclusion of an in-frame exon with a premature termination codon, is another possible correcting mechanism.[30–33] Recently, a nonsense mutation in *CEP290* that causes blindness has been shown to induce exon skipping and to lead to a relatively mild retinal phenotype.[34] Because the skipping of *GPR180* exon 2 would not disrupt the open reading frame, NAS could explain why the p.Gln115* substitution is not as detrimental as gene ablation.

The p.Gln115* substitution was not reported in the Exome Aggregator database (ExAC), Exome Variant Server (EVS), 1000 Genomes, or dbSNP datasets. However, we identified in the ExAC database 12 other rare variants that might cause protein truncation (six nonsense and six frameshift mutations, 0.00004 < minor allele frequency < 0.000008; Table S5). Provided that these variants are confirmed, studying their molecular consequence at the mRNA and/or the protein levels and knowing the ophthalmologic status of carrier individuals will certainly help in understanding the role of *GPR180* in MCOR and goniodysgenesis. Meanwhile, to address this important question, we screened the *GPR180* exome for mutations in a series of individuals having an eye disease with goniodysgenesis, including ten individuals with Axenfeld-Rieger anomaly or Peters anomaly (MIM 604229) and no *PAX6*, *PITX2*, *FOXC1*, *CYP1B1*, *MAF*, or *MYOC* mutation (n = 5 and n = 5, respectively), and 11 index cases of primary congenital glaucoma (n = 9) or juvenile glaucoma (n = 2) with no *CYP1B1* mutations. Primer sequences are given in Table S6. No *GPR180* candidate disease variants were identified in *GPR180* exon and intron-exon boundaries in any of the individuals.

Despite strong arguments in favor of the involvement of GPR180 in MCOR, in the absence of 13q32.1 deletions that do not disrupt *TGDS* or of a *GPR180* mutation that causes the full MCOR phenotype, we cannot formally exclude that haploinsufficiency of *GPR180* is necessary, but not sufficient, for MCOR to manifest.

The second gene lost or disrupted in MCOR-affected individuals, *TGDS*, encodes the dTDP-D-glucose 4,6-dehydratase, an evolutionarily conserved NAD-dependent sugar epimerase/dehydratase of the short chain dehydrogenase/reductase extended-type family (SDR2E1, EC:4.2.1.46). In human, SDR enzymes display a wide substrate spectrum, ranging from steroids, alcohols, sugars, and aromatic compounds to xenobiotics.[35] TGDS catalyzes the dehydration of dTDP-alpha-D-glucose into dTDP-4-dehydro-6-deoxy-alpha-D-glucose. It contributes to deoxysugar metabolism,[35,36] but its exact function is unknown. In bacteria, TGDS is essential to the biogenesis of cell envelope components and antibiotics,[37] and in *C. elegans*, it is required for normal growth rates, larval development and survival, reproduction, and coordinated locomotion.[38] In human eyes, *TGDS* expression is lower than that of *GPR180*, and unlike *GPR180*, it has no preferential expression in the iris.[26] More importantly, very recently, biallelic *TGDS* mutations have been reported to cause Catel-Manzke syndrome (MIM 302380), which is characterized by Pierre Robin sequence (MIM 261800; HP:0000201) and a unique form of bilateral hyperphalangy causing clinodactyly of the index finger (HP:0009467).[39] Neither the affected individuals nor their heterozygote parents are reported to have eye disease.[39] Therefore, it is unlikely that TGDS dysfunction in human is responsible for MCOR.

Finally, it cannot be excluded that full range of MCOR symptoms are due to both the loss of GPR180 function and to that of elements that regulate the expression of neighboring genes by position effect. Inspection of the ENCODE repository for transcription factor-binding site identified

by ChIP-seq detected no eye-specific binding sites in the 35.3 kbp sequence of the shortest MCOR deletion (Figure S12). Likewise, inspection of the database of conserved non-coding orthologous regions (CONDOR) identified no highly conserved non-coding elements (HCNE) in the 35.3 kbp MCOR minimal region. However, two genes involved in eye development are located close to the MCOR region, namely *DCT* (MIM 191275), which encodes the dopachrome tautomerase, and *SOX21* (MIM 604974), which encodes SRY-related high-mobility-group box 21.

DCT is located 110 kbp upstream of proximal boundary of the minimal interval (Figure 2). DCT functions downstream of tyrosinase (TYR [MIM 606933]) and tyrosinase-related protein-1 (TRP1 [MIM 115501]) in the biosynthetic pathway of eumelanin in pigment cells. In the mouse, *Dct* mutations cause the Slaty phenotype in which the iris is normal in the first months of life. Later on, age-related dispersed pigment across the surface of the iris combined with mild transillumination is noted.[40] To our knowledge, no *DCT* mutation is reported in human disease so far but ten loss-of-function alleles are described in EVS. One of these variants, p.Tyr75Serfs*50 is homozygous in 12/6,249 individuals, making unlikely a contribution of DCT loss of function in MCOR. However, considering that pigmentation has a role on the development of the neuroretina,[41,42] it cannot be excluded that 13q32.1 deletions cause *DTC* overexpression and dysregulate iris development mechanisms.

SOX21 is located 75 kbp upstream of the distal boundary of the minimal MCOR interval (Figure 2). SOX21 has been reported to be a general mediator of the effects of SOX2,[43] whose interaction with PAX6 is crucial to coordinate eye development.[44] It is known to be expressed in the developing lens in chickens[45] and zebrafish.[46] Additionally, *sox21b* knock-down in the zebrafish causes lens malformation.[47] In the mouse, complete inactivation of *Sox21* has been reported to cause cyclic alopecia,[48] but the ocular phenotype of the animal is unknown. Altered regulation of *SOX21* expression in MCOR-affected individuals cannot be excluded.

In summary, here we report heterozygote 13q32.1 deletions in 6/6 MCOR-affected families of variable ethnic origin, which invariably encompass *GPR180* and *TGDS*. We suggest that *GPR180* ablation, alone or in combination with the loss of elements that regulate the expression of neighboring genes by position effect, is the cause of the disease. Further studies will hopefully allow the identification of the molecular mechanisms underlying this rare disease. It should provide further insights into the development of the anterior chamber of the eye, whose anomalies are an important cause of visual loss due to glaucoma.

Accession Numbers

The accession number for the copy-number variants in the DECIPHER database are 301464, 301465, 301468, 301469, 301471, and 301472.

Supplemental Data

Supplemental Data include 12 figures and 6 tables and can be found with this article online at http://dx.doi.org/10.1016/j.ajhg.2015.01.014.

Acknowledgments

We are grateful to the families for their participation in the study. We thank Johan Castille and Gérard Pivert for technical assistance. This work was supported by grants from the Fédération des Aveugles de France (FAF) to L.F.-T., Retina France to J.-M.R., Geniris to J.-M.R. and P.C., the Ministry of Education, Culture, Sport, Science and Technology of Japan Grant-in-aid N°20592067 to A.T., and the Conde de Valenciana Foundation patronage to A.R.-M. and J.C.Z.

Received: October 8, 2014
Accepted: January 20, 2015
Published: March 12, 2015

Web Resources

The URLs for data presented herein are as follows:

1000 Genomes, http://browser.1000genomes.org
CONDOR, http://condor.nimr.mrc.ac.uk/
Database of Genomic Variants (DGV), http://dgv.tcag.ca/dgv/app/home
dbSNP, http://www.ncbi.nlm.nih.gov/projects/SNP/
DECIPHER, http://decipher.sanger.ac.uk/
ExAC Browser, http://exac.broadinstitute.org/
NHLBI Exome Sequencing Project (ESP) Exome Variant Server, http://evs.gs.washington.edu/EVS/
OMIM, http://www.omim.org/
RefSeq, http://www.ncbi.nlm.nih.gov/RefSeq
UCSC Genome Browser, http://genome.ucsc.edu

References

1. Butler, J.M., Raviola, G., Miller, C.D., and Friedmann, A.I. (1989). Fine structural defects in a case of congenital microcoria. Graefes Arch. Clin. Exp. Ophthalmol. *227*, 88–94.
2. Simpson, W.A., and Parsons, M.A. (1989). The ultrastructural pathological features of congenital microcoria. A case report. Arch. Ophthalmol. *107*, 99–102.
3. Pietropaolo, A., Corvino, C., DeBlasi, A., and Calabrò, F. (1998). Congenital microcoria: case report and histological study. J. Pediatr. Ophthalmol. Strabismus *35*, 125–127.
4. Ramirez-Miranda, A., Paulin-Huerta, J.M., Chavez-Mondragón, E., Islas-de la Vega, G., and Rodriguez-Reyes, A. (2011). Ultrabiomicroscopic-histopathologic correlations in individuals with autosomal dominant congenital microcoria: three-generation family report. Case Rep. Ophthalmol. *2*, 160–165.
5. Toulemont, P.J., Urvoy, M., Coscas, G., Lecallonnec, A., and Cuvilliers, A.F. (1995). Association of congenital microcoria with myopia and glaucoma. A study of 23 patients with congenital microcoria. Ophthalmology *102*, 193–198.
6. Tawara, A., Itou, K., Kubota, T., Harada, Y., Tou, N., and Hirose, N. (2005). Congenital microcoria associated with late-onset developmental glaucoma. J. Glaucoma *14*, 409–413.

7. Mazzeo, V., Gaiba, G., and Rossi, A. (1986). Hereditary cases of congenital microcoria and goniodysgenesis. Ophthalmic Paediatr. Genet. *7*, 121–125.
8. Tawara, A., and Inomata, H. (1983). Familial cases of congenital microcoria associated with late onset congenital glaucoma and goniodysgenesis. Jpn. J. Ophthalmol. *27*, 63–72.
9. Rouillac, C., Roche, O., Marchant, D., Bachner, L., Kobetz, A., Toulemont, P.J., Orssaud, C., Urvoy, M., Odent, S., Le Marec, B., et al. (1998). Mapping of a congenital microcoria locus to 13q31-q32. Am. J. Hum. Genet. *62*, 1117–1122.
10. Ardouin, M., Urvoy, M., and Lefranc, J. (1964). Microcorie congénitale. Bull. Mem. Soc. Fr. Ophtalmol. *77*, 356.
11. Ramprasad, V.L., Sripriya, S., Ronnie, G., Nancarrow, D., Saxena, S., Hemamalini, A., Kumar, D., Vijaya, L., and Kumaramanickavel, G. (2005). Genetic homogeneity for inherited congenital microcoria loci in an Asian Indian pedigree. Mol. Vis. *11*, 934–940.
12. Bremner, F.D., Houlden, H., and Smith, S.E. (2004). Genotypic and phenotypic heterogeneity in familial microcoria. Br. J. Ophthalmol. *88*, 469–473.
13. Saugier-Veber, P., Goldenberg, A., Drouin-Garraud, V., de La Rochebrochard, C., Layet, V., Drouot, N., Le Meur, N., Gilbert-Du-Ssardier, B., Joly-Hélas, G., Moirot, H., et al. (2006). Simple detection of genomic microdeletions and microduplications using QMPSF in patients with idiopathic mental retardation. Eur. J. Hum. Genet. *14*, 1009–1017.
14. Stankiewicz, P., and Lupski, J.R. (2002). Genome architecture, rearrangements and genomic disorders. Trends Genet. *18*, 74–82.
15. Vissers, L.E., Bhatt, S.S., Janssen, I.M., Xia, Z., Lalani, S.R., Pfundt, R., Derwinska, K., de Vries, B.B., Gilissen, C., Hoischen, A., et al. (2009). Rare pathogenic microdeletions and tandem duplications are microhomology-mediated and stimulated by local genomic architecture. Hum. Mol. Genet. *18*, 3579–3593.
16. Verdin, H., D'haene, B., Beysen, D., Novikova, Y., Menten, B., Sante, T., Lapunzina, P., Nevado, J., Carvalho, C.M., Lupski, J.R., and De Baere, E. (2013). Microhomology-mediated mechanisms underlie non-recurrent disease-causing microdeletions of the FOXL2 gene or its regulatory domain. PLoS Genet. *9*, e1003358.
17. Lieber, M.R. (2008). The mechanism of human nonhomologous DNA end joining. J. Biol. Chem. *283*, 1–5.
18. Lee, J.A., Carvalho, C.M., and Lupski, J.R. (2007). A DNA replication mechanism for generating nonrecurrent rearrangements associated with genomic disorders. Cell *131*, 1235–1247.
19. Hastings, P.J., Ira, G., and Lupski, J.R. (2009). A microhomology-mediated break-induced replication model for the origin of human copy number variation. PLoS Genet. *5*, e1000327.
20. Chen, J.M., Chuzhanova, N., Stenson, P.D., Férec, C., and Cooper, D.N. (2005). Complex gene rearrangements caused by serial replication slippage. Hum. Mutat. *26*, 125–134.
21. Sheen, C.R., Jewell, U.R., Morris, C.M., Brennan, S.O., Férec, C., George, P.M., Smith, M.P., and Chen, J.M. (2007). Double complex mutations involving F8 and FUNDC2 caused by distinct break-induced replication. Hum. Mutat. *28*, 1198–1206.
22. Tsukada, S., Iwai, M., Nishiu, J., Itoh, M., Tomoike, H., Horiuchi, M., Nakamura, Y., and Tanaka, T. (2003). Inhibition of experimental intimal thickening in mice lacking a novel G-protein-coupled receptor. Circulation *107*, 313–319.
23. Milligan, G. (2008). A day in the life of a G protein-coupled receptor: the contribution to function of G protein-coupled receptor dimerization. Br. J. Pharmacol. *153* (1), S216–S229.
24. Iida, A., Tanaka, T., and Nakamura, Y. (2003). High-density SNP map of human ITR, a gene associated with vascular remodeling. J. Hum. Genet. *48*, 170–172.
25. Shyamsundar, R., Kim, Y.H., Higgins, J.P., Montgomery, K., Jorden, M., Sethuraman, A., van de Rijn, M., Botstein, D., Brown, P.O., and Pollack, J.R. (2005). A DNA microarray survey of gene expression in normal human tissues. Genome Biol. *6*, R22.
26. Wagner, A.H., Anand, V.N., Wang, W.H., Chatterton, J.E., Sun, D., Shepard, A.R., Jacobson, N., Pang, I.H., Deluca, A.P., Casavant, T.L., et al. (2013). Exon-level expression profiling of ocular tissues. Exp. Eye Res. *111*, 105–111.
27. Lai, Y.L. (1972). The development of the dilator muscle in the iris of the albino rat. Exp. Eye Res. *14*, 203–207.
28. Lai, Y.L. (1972). The development of the sphincter muscle in the iris of the albino rat. Exp. Eye Res. *14*, 196–202.
29. Jungreis, I., Lin, M.F., Spokony, R., Chan, C.S., Negre, N., Victorsen, A., White, K.P., and Kellis, M. (2011). Evidence of abundant stop codon readthrough in *Drosophila* and other metazoa. Genome Res. *21*, 2096–2113.
30. Dietz, H.C., Valle, D., Francomano, C.A., Kendzior, R.J., Jr., Pyeritz, R.E., and Cutting, G.R. (1993). The skipping of constitutive exons in vivo induced by nonsense mutations. Science *259*, 680–683.
31. Valentine, C.R. (1998). The association of nonsense codons with exon skipping. Mutat. Res. *411*, 87–117.
32. Cartegni, L., Chew, S.L., and Krainer, A.R. (2002). Listening to silence and understanding nonsense: exonic mutations that affect splicing. Nat. Rev. Genet. *3*, 285–298.
33. Wang, J., Chang, Y.F., Hamilton, J.I., and Wilkinson, M.F. (2002). Nonsense-associated altered splicing: a frame-dependent response distinct from nonsense-mediated decay. Mol. Cell *10*, 951–957.
34. Littink, K.W., Pott, J.W., Collin, R.W., Kroes, H.Y., Verheij, J.B., Blokland, E.A., de Castro Miró, M., Hoyng, C.B., Klaver, C.C., Koenekoop, R.K., et al. (2010). A novel nonsense mutation in CEP290 induces exon skipping and leads to a relatively mild retinal phenotype. Invest. Ophthalmol. Vis. Sci. *51*, 3646–3652.
35. Kallberg, Y., Oppermann, U., Jörnvall, H., and Persson, B. (2002). Short-chain dehydrogenase/reductase (SDR) relationships: a large family with eight clusters common to human, animal, and plant genomes. Protein Sci. *11*, 636–641.
36. Persson, B., Kallberg, Y., Bray, J.E., Bruford, E., Dellaporta, S.L., Favia, A.D., Duarte, R.G., Jörnvall, H., Kavanagh, K.L., Kedishvili, N., et al. (2009). The SDR (short-chain dehydrogenase/reductase and related enzymes) nomenclature initiative. Chem. Biol. Interact. *178*, 94–98.
37. Allard, S.T.M., Beis, K., Giraud, M.F., Hegeman, A.D., Gross, J.W., Wilmouth, R.C., Whitfield, C., Graninger, M., Messner, P., Allen, A.G., et al. (2002). Toward a structural understanding of the dehydratase mechanism. Structure *10*, 81–92.
38. Levin, M., Hashimshony, T., Wagner, F., and Yanai, I. (2012). Developmental milestones punctuate gene expression in the *Caenorhabditis* embryo. Dev. Cell *22*, 1101–1108.
39. Ehmke, N., Caliebe, A., Koenig, R., Kant, S.G., Stark, Z., Cormier-Daire, V., Wieczorek, D., Gillessen-Kaesbach, G., Hoff, K., Kawalia, A., et al. (2014). Homozygous and compound-heterozygous mutations in TGDS cause Catel-Manzke syndrome. Am. J. Hum. Genet. *95*, 763–770.

40. Anderson, M.G., Hawes, N.L., Trantow, C.M., Chang, B., and John, S.W. (2008). Iris phenotypes and pigment dispersion caused by genes influencing pigmentation. Pigment Cell Melanoma Res *21*, 565–578.
41. Grønskov, K., Ek, J., and Brondum-Nielsen, K. (2007). Oculocutaneous albinism. Orphanet J. Rare Dis. *2*, 43.
42. Bhansali, P., Rayport, I., Rebsam, A., and Mason, C. (2014). Delayed neurogenesis leads to altered specification of ventrotemporal retinal ganglion cells in albino mice. Neural Dev. *9*, 11.
43. Kuzmichev, A.N., Kim, S.K., D'Alessio, A.C., Chenoweth, J.G., Wittko, I.M., Campanati, L., and McKay, R.D. (2012). Sox2 acts through Sox21 to regulate transcription in pluripotent and differentiated cells. Curr. Biol. *22*, 1705–1710.
44. Matsushima, D., Heavner, W., and Pevny, L.H. (2011). Combinatorial regulation of optic cup progenitor cell fate by SOX2 and PAX6. Development *138*, 443–454.
45. Uchikawa, M., Kamachi, Y., and Kondoh, H. (1999). Two distinct subgroups of Group B Sox genes for transcriptional activators and repressors: their expression during embryonic organogenesis of the chicken. Mech. Dev. *84*, 103–120.
46. Lan, X., Wen, L., Li, K., Liu, X., Luo, B., Chen, F., Xie, D., and Kung, H.F. (2011). Comparative analysis of duplicated sox21 genes in zebrafish. Dev. Growth Differ. *53*, 347–356.
47. Pauls, S., Smith, S.F., and Elgar, G. (2012). Lens development depends on a pair of highly conserved Sox21 regulatory elements. Dev. Biol. *365*, 310–318.
48. Kiso, M., Tanaka, S., Saba, R., Matsuda, S., Shimizu, A., Ohyama, M., Okano, H.J., Shiroishi, T., Okano, H., and Saga, Y. (2009). The disruption of Sox21-mediated hair shaft cuticle differentiation causes cyclic alopecia in mice. Proc. Natl. Acad. Sci. USA *106*, 9292–9297.